Karlsruhe Institute of Technology

On the determination of atmospheric boundary layer structures by ground-based remote sensing (SODAR, lidar/ceilometer, RASS)

Stefan Emeis
stefan.emeis@kit.edu

INSTITUTE OF METEOROLOGY AND CLIMATE RESEARCH, Atmospheric Environmental Research

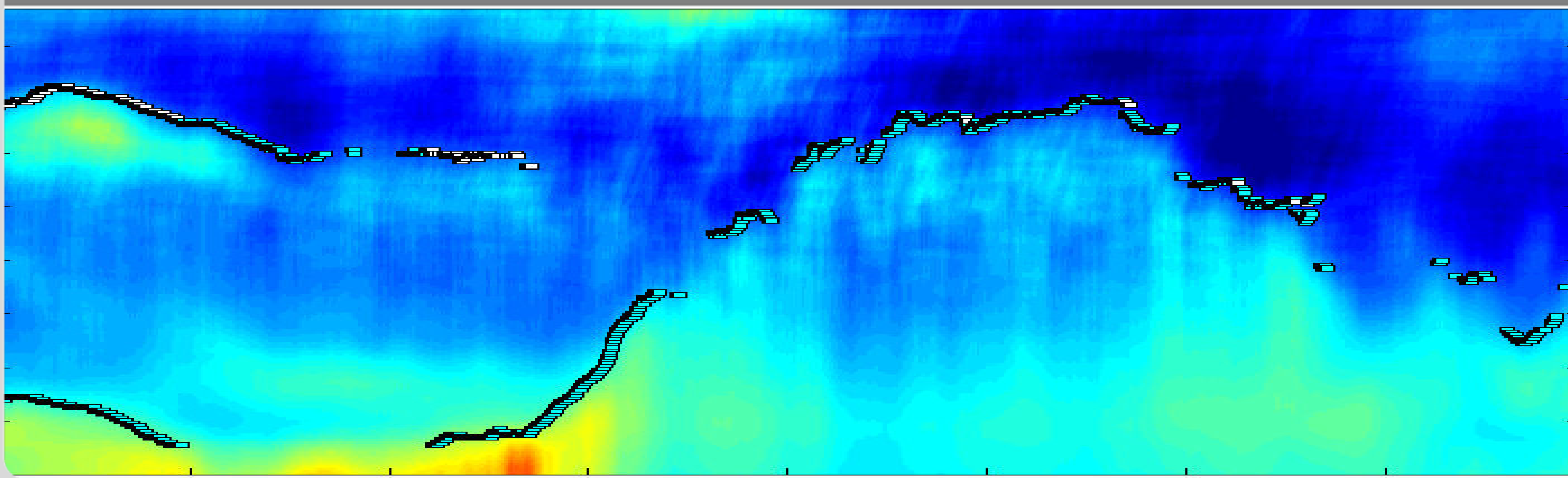

Introduction

-features of the atmospheric boundary layer

-detection techniques

 stefan.emeis@kit.edu Institute for Meteorology and Climate Research – Atmospheric Environmental Research

diurnal variation of PBL

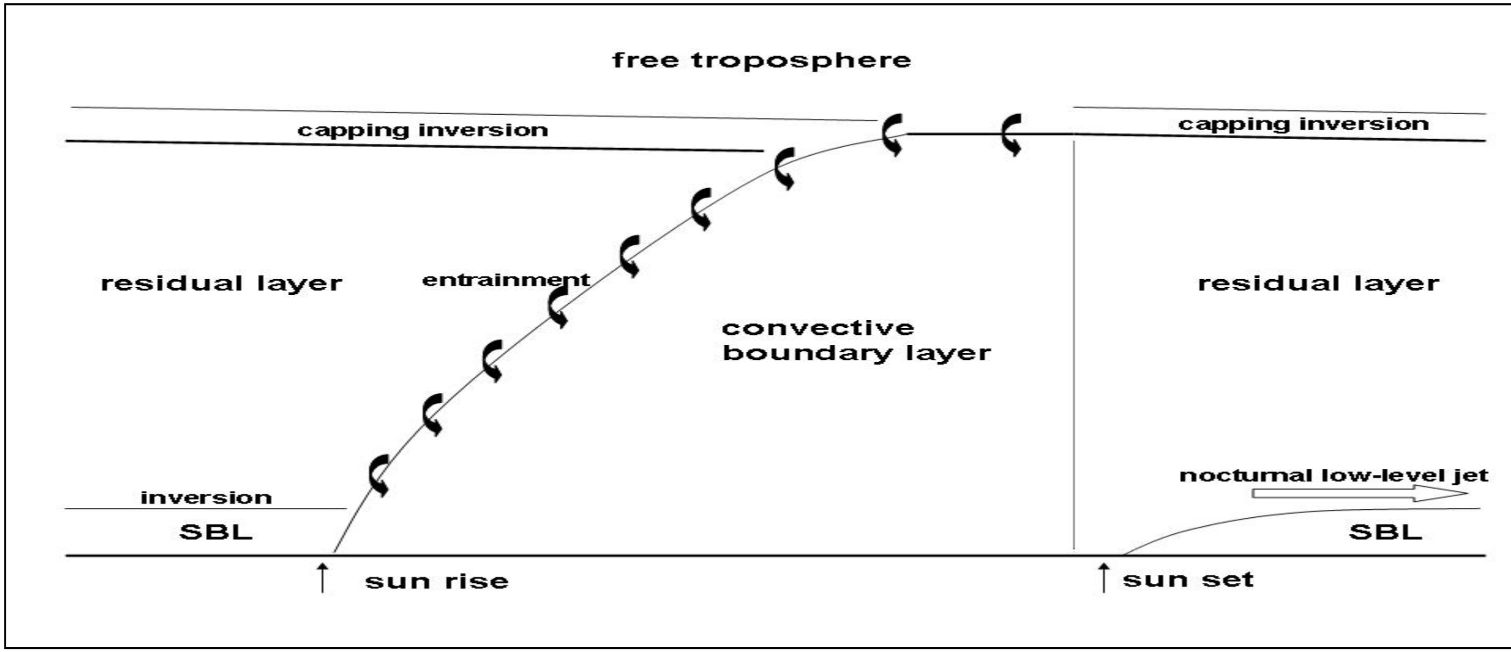

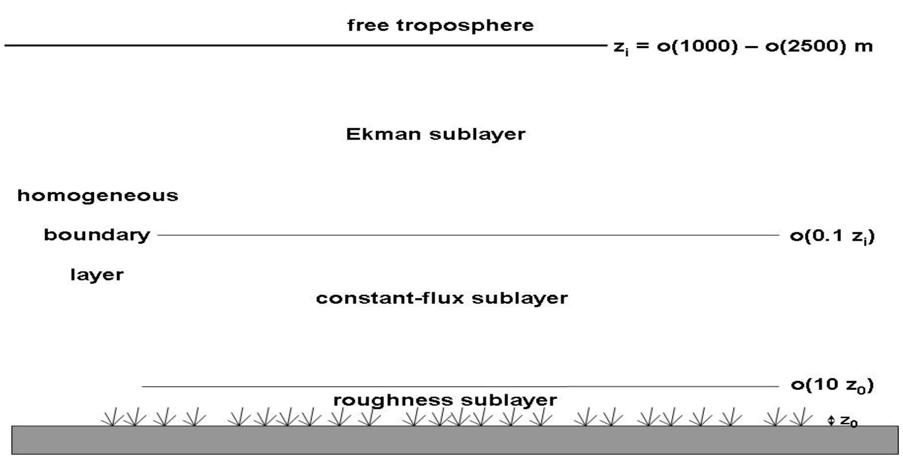

vertical structure of PBL

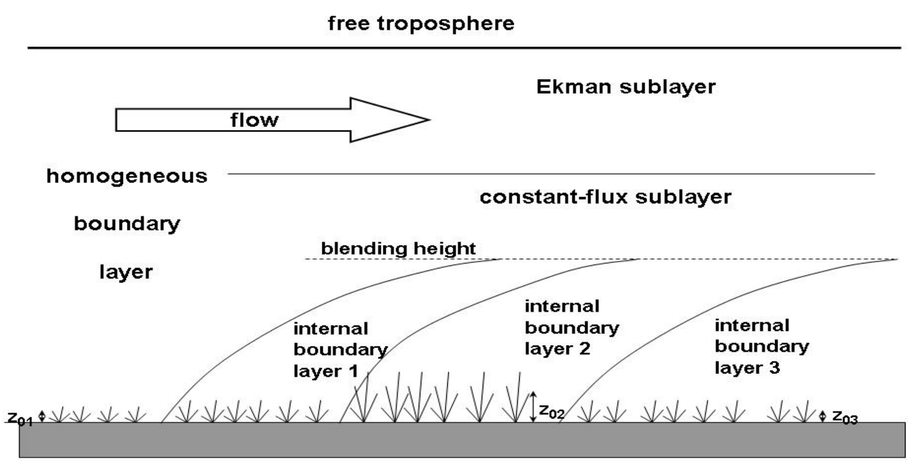

internal layers in PBL

special types of PBL

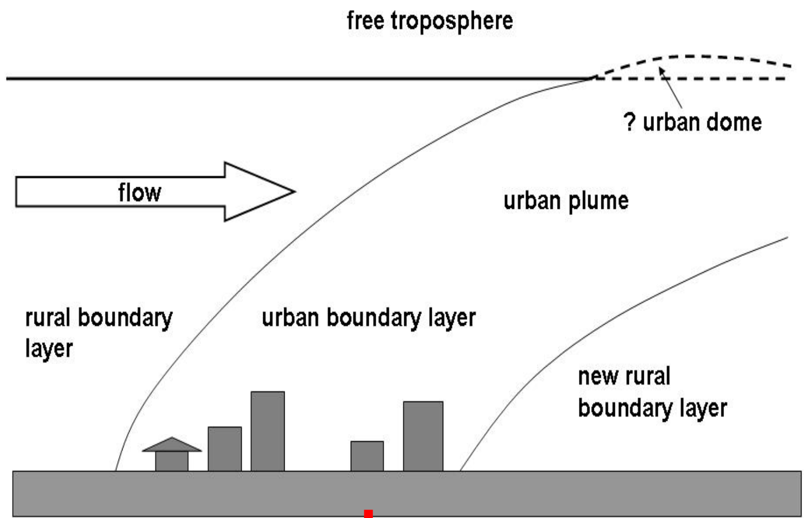

urban

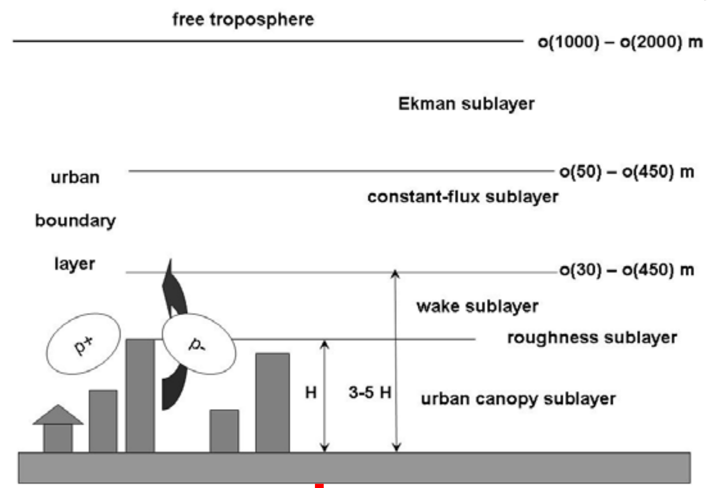

urban

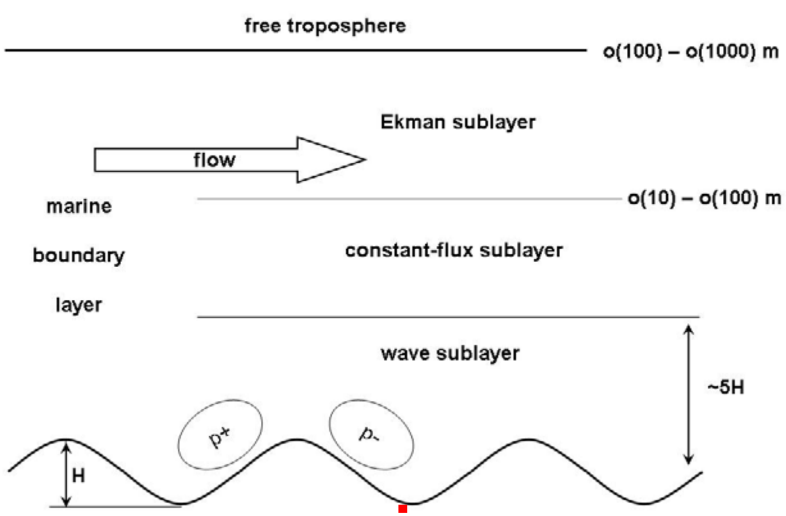

marine

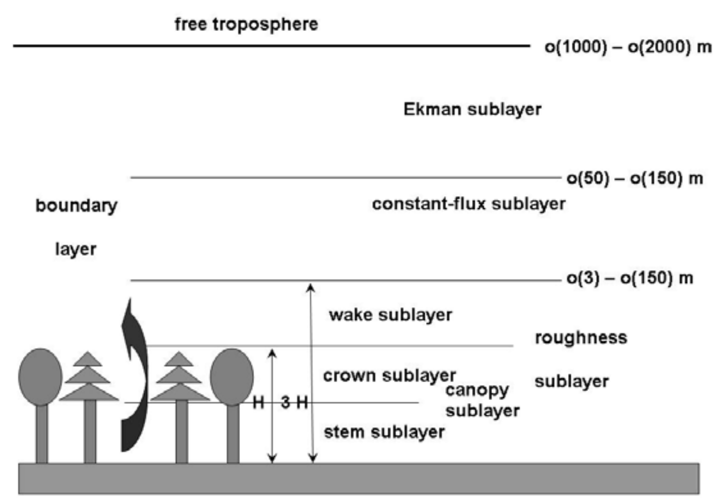

forest

Basic remote sensing techniques

subject of this lecture

name	princple	spatial resolution	direction	type
RADAR	backscatter, electro-magnetic pulses, fixed wave length	profiling	scanning, slanted	active, monostatic
SODAR	backscatter, acoustic pulses, fixed wave length	profiling	fixed, slanted, vertical	active, usually monostatic
LIDAR	backscatter, optical pulses, fixed wave length(s)	profiling	scanning, fixed, horizontal, slanted, vertical	active, monostatic
RASS	backscatter, acoustic, electro-magnetic, fixed wave length	profiling	fixed, vertical	active, monostatic
FTIR	absorption, infrared, spectrum	path-averaging	fixed, horizontal, slanted	active, bistatic or passive
FTIR	emission, infrared, spectrum	path-averaging	fixed, horizontal, slanted	passive
DOAS	absorption, optical, fixed wave lengths	path-averaging	fixed, horizontal	active, bistatic
radiometry	electro-magnetic, fixed wave length(s)	averaging, profiling	fixed, scanning, slanted, vertical	passive
tomography	travel time, acoustic, fixed wave length	horizontal distribution	fixed, horizontal	active, multiple emitters and receivers

subject of this lecture

Frequencies for atmospheric remote sensing

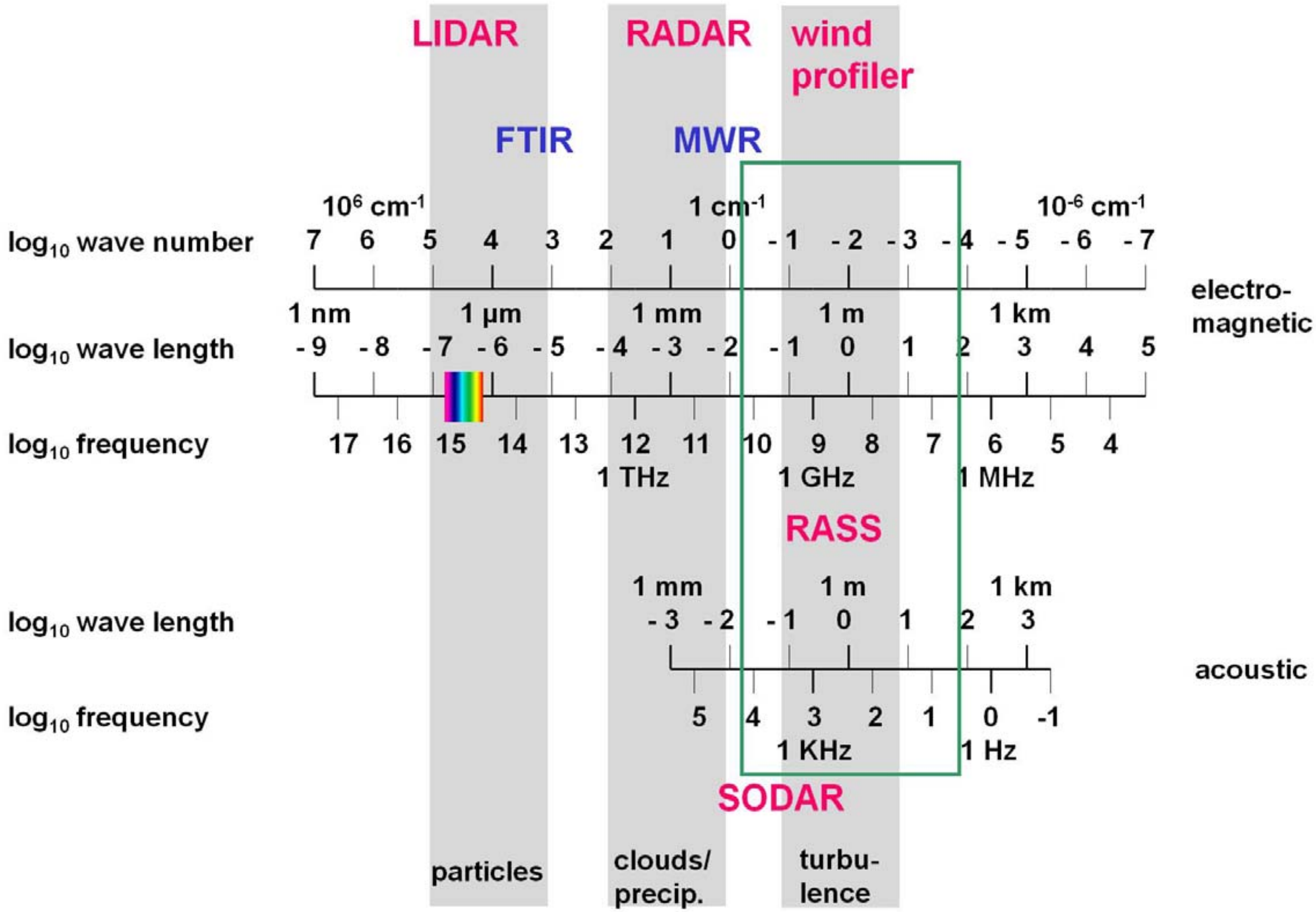

Emeis, S., 2010: Measurement Methods in Atmospheric Sciences - In situ and remote. Borntraeger, Stuttgart, 272 pp., 103 figs, 28 tables, ISBN 978-3-443-01066-9.

SODAR

wind, turbulence, temperature gradients, mixing-layer height

stefan.emeis@kit.edu Institute for Meteorology and Climate Research – Atmospheric Environmental Research

monostatic SODAR: measuring principles

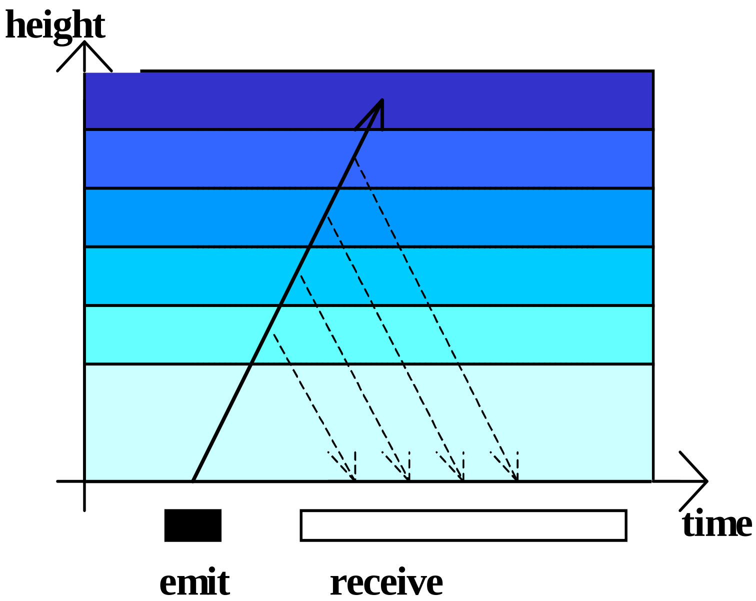

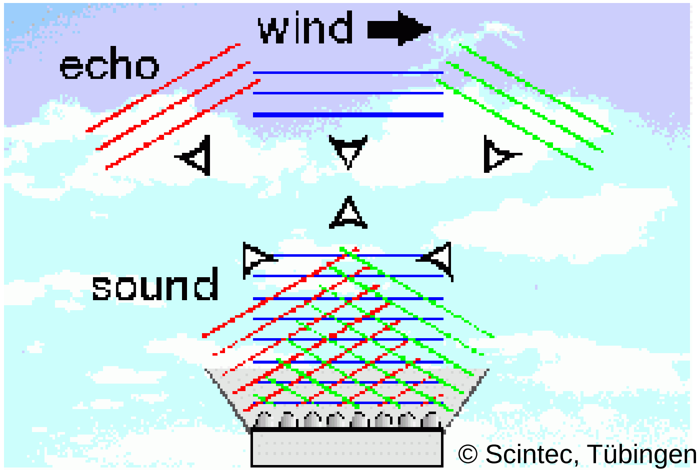

deduction:

sound travel time	=	height
backscatter intensity	=	turbulence
Doppler-shift	=	wind speed

Emission of sound waves into three directions:

in order to measure all three components of the wind (horizontal and vertical)

stefan.emeis@kit.edu Institute for Meteorology and Climate Research – Atmospheric Environmental Research

The SODAR equation:

$$P_R = r^{-2}\,(c_s \tau A \varepsilon / 2)\, P_0\, \beta_s\, e^{-2\sigma r} + P_{bg}$$

P_R received power,
P_0 emitted power,
ε antenna efficiency,
A effective antenna area,
σ sound absorption in air due to classical and molecular absorption due to the collision of water molecules with the oxygen and nitrogen molecules of the air,
r distance between the scattering volume and the instrument,
τ pulse duration (typically between 20 and 100 ms),
β_s backscattering cross-section (typically in the order of 10^{-11} m^{-1} sr^{-1}),
c_s sound speed,
P_{bg} background noise.

Emitted power: ~ 10^3 W, received (backscattered) power: 10^{-15} W

stefan.emeis@kit.edu Institute for Meteorology and Climate Research – Atmospheric Environmental Research

The SODAR equation:

$$P_R = r^{-2} (c_s \tau A \varepsilon/2)\, P_0\, \beta_s\, e^{-2\sigma r} + P_{bg}$$

The ratio of the two terms on the right-hand side of the SODAR equation is called signal-to-noise ratio (usually abbreviated as SNR).

The backscattering cross-section β_s is a function of the temperature structure function C_T^2 (Tatarskii 1961).

For a monostatic SODAR we find (Reitebuch 1999) when using the wave number k = 2π/λ:

$$\beta_s(180°) = 0{,}00408\, k^{1/3}\, C_T^2 / T^2$$

Reitebuch, O., 1999: SODAR-Signalverarbeitung von Einzelpulsen zur Bestimmung hochaufgelöster Windprofile. Schriftenreihe des Fraunhofer-Instituts für Atmosphärische Umweltforschung, Shaker Verlag GmbH Aachen, Bd. 62, 178 S.

Tatarskii, V.I., 1971: The effect of the turbulent atmosphere on wave propagation. Kefer Press, Jerusalem, 472 S.

Großes SODAR
des IMK-IFU
(METEK DSDR3x7)

Frequenz: 1500 Hz
Reichweite: 1300 m
Auflösung: 20 m
unterste
Messhöhe: ca. 60 m

Höhe: 4 m
Breite: 1,50 m
Länge: 10 m
Gewicht: 8 t

SODAR sample plot (diurnal evolution, low-level jet)

horizontal wind speed and direction

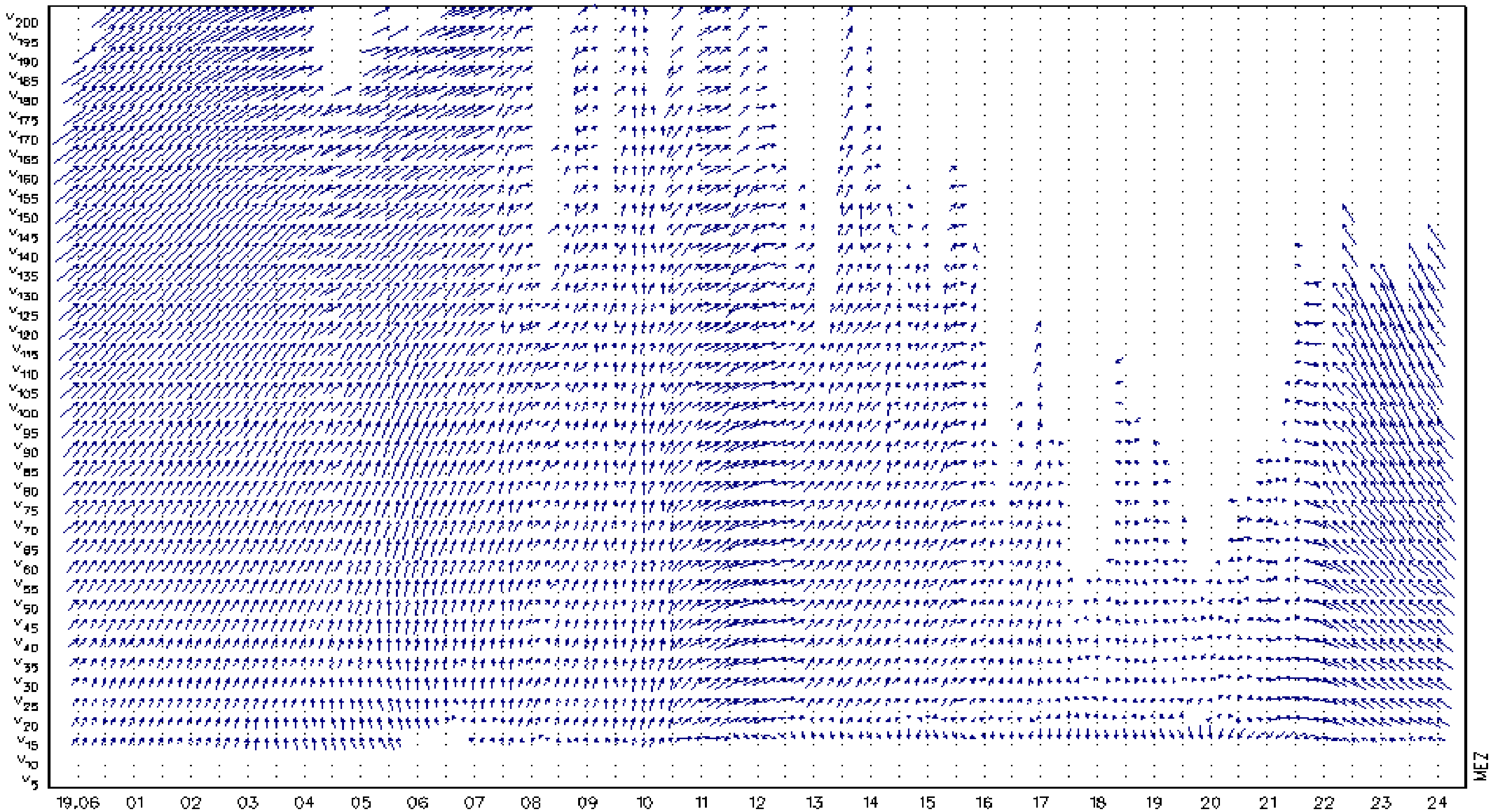

Abb.: 10'–Mittel des Windvektors (v_x) für ausgewählte Höhen (x)
IFU–MiniSODAR Sachsen–Anhalt Juni 1999

→ = 3 m/s Westwind

IFU GAP

SODAR sample plot (daytime convective BL)

acoustic backscatter intensity **sigma w**

40 – 300 m

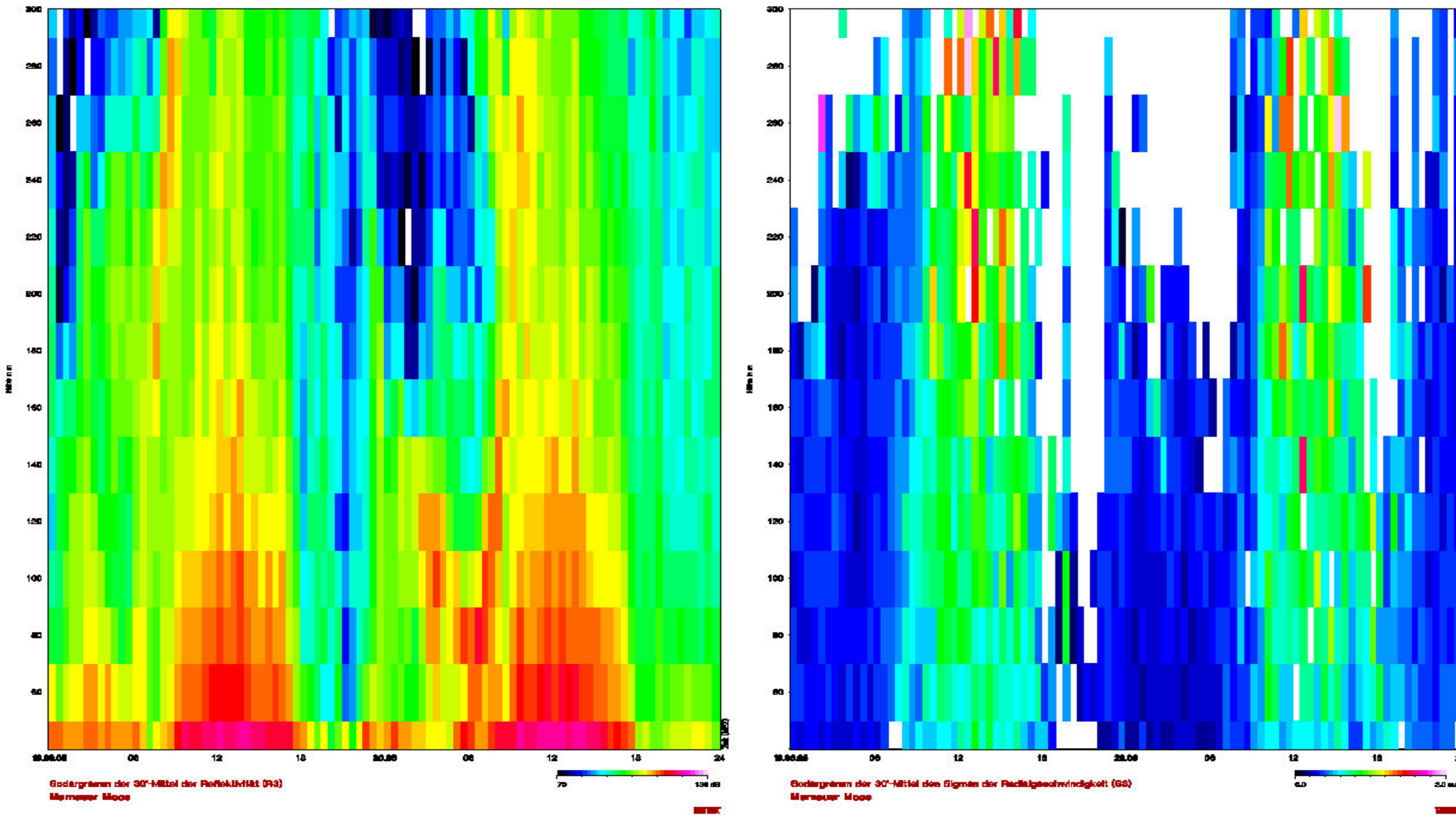

2 days, midnight to midnight

stefan.emeis@kit.edu Institute for Meteorology and Climate Research – Atmospheric Environmental Research

SODAR sample plot (lifted inversion)

40 – 400 m

acoustic backscatter intensity

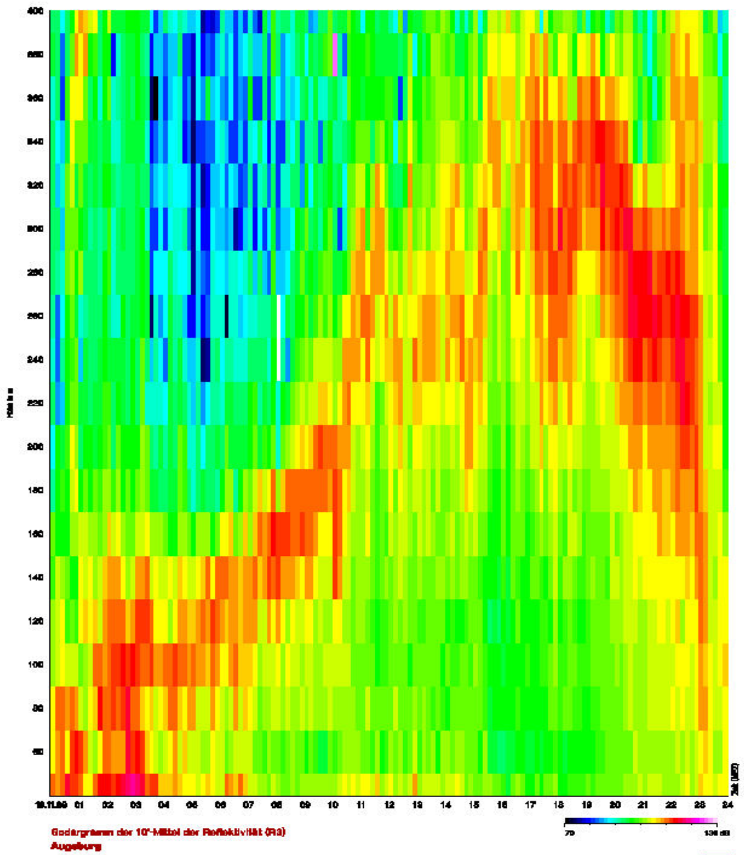

sigma w

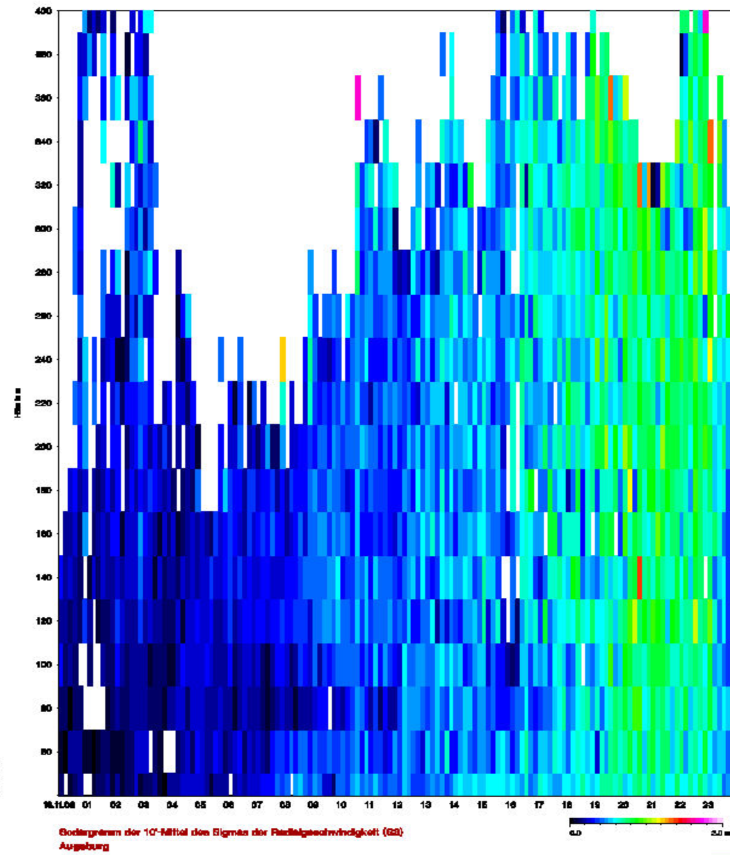

1 day, midnight to midnight

Algorithms to detect MLH from SODAR data

criterion 1:
upper edge of high turbulence

criterion 2:
surface and lifted inversions

MLH = Min (C1, C2)

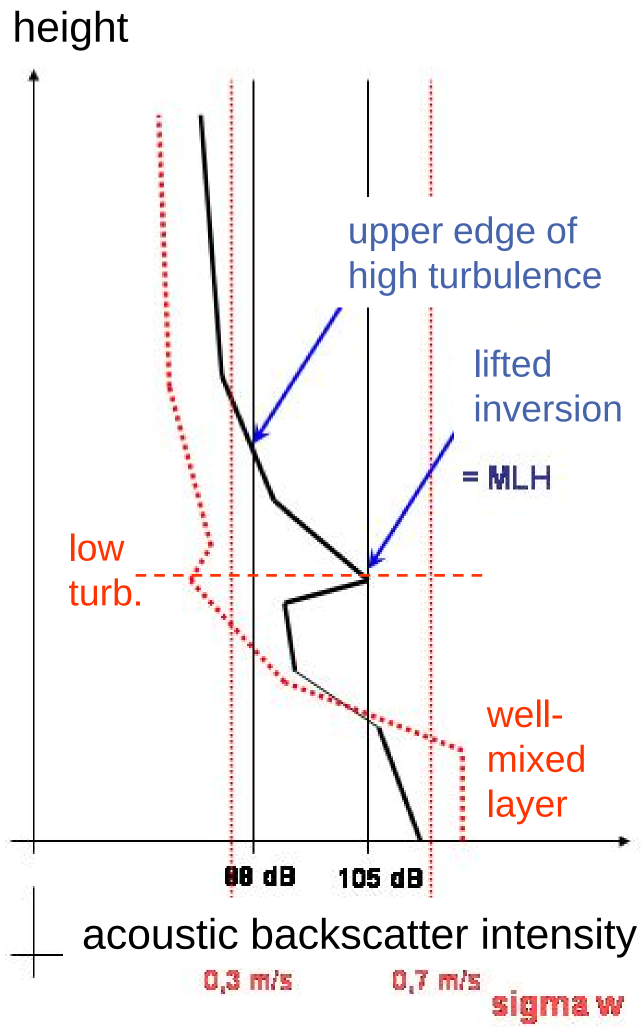

example 1: daytime

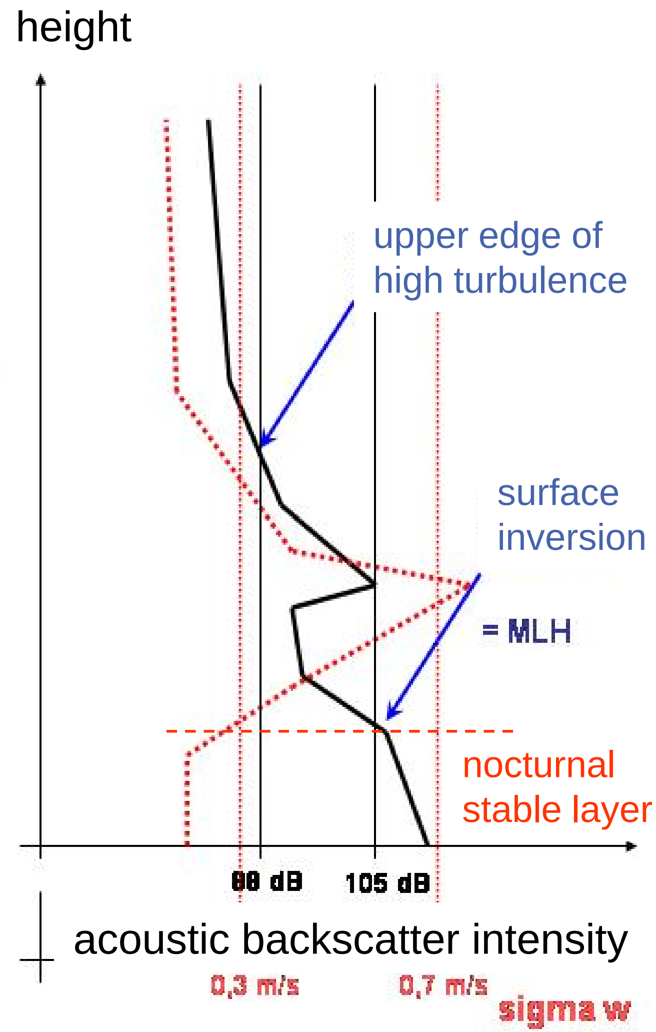

example 2: night-time

stefan.emeis@kit.edu Institute for Meteorology and Climate Research – Atmospheric Environmental Research

Ceilometer

aerosol detection, mixing-layer height

stefan.emeis@kit.edu Institute for Meteorology and Climate Research –
Atmospheric Environmental Research

Ceilometer/LIDAR measuring principle

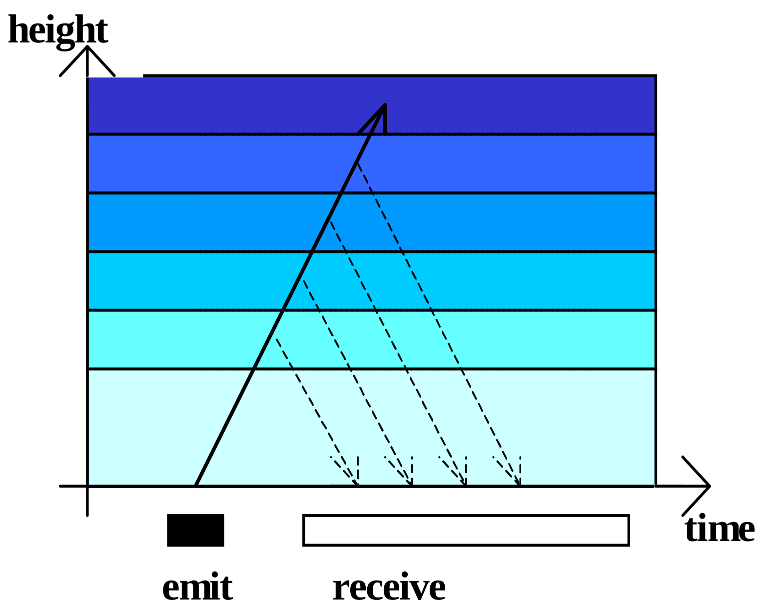

detection:

travel time of signal = height
backscatter intensity = particle size and number distribution
Doppler-shift = cannot be analyzed from ceilometer data
(available only from a Wind-LIDAR: velocity component in line of sight)

The LIDAR equation:

$$P_R(\lambda,r) = r^{-2}\ (c\tau A\varepsilon/2)\ P_0\ [\beta_m(\lambda,r) + \beta_p(\lambda,r)]\ e^{-2\sigma r} + P_{bg}$$

- r distance between the LIDAR and the backscattering object,
- c speed of light,
- τ pulse duration,
- A antenna area,
- ε correction term for the detector efficiency and losses due to the lenses,
- P_0 emitted energy,
- β_m backscatter coefficient for molecules
- β_p backscatter coefficient for particles,
- σ absorption of light in the atmosphere,
- P_{bg} background noise.

For a ceilometer β_m is negligible and only β_p is important

stefan.emeis@kit.edu Institute for Meteorology and Climate Research – Atmospheric Environmental Research

ceilometer sample plot (daytime convective BL)

optical backscatter intensity

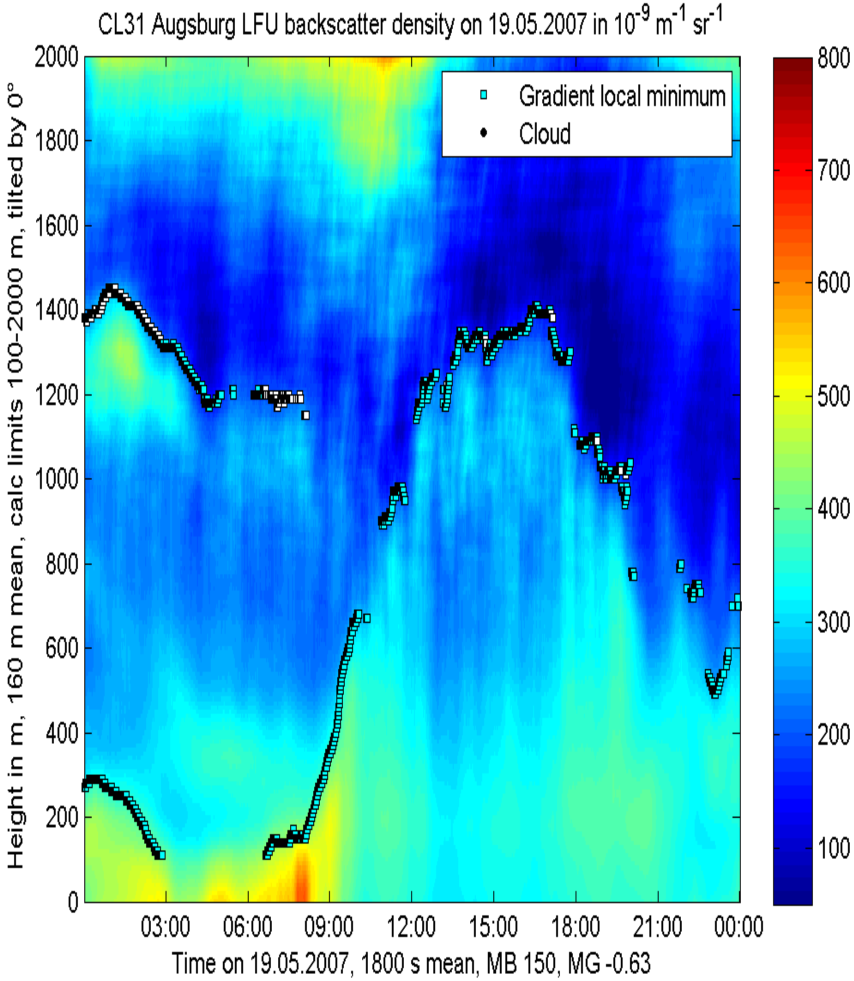

negative vertical gradient of optical backscatter intensity

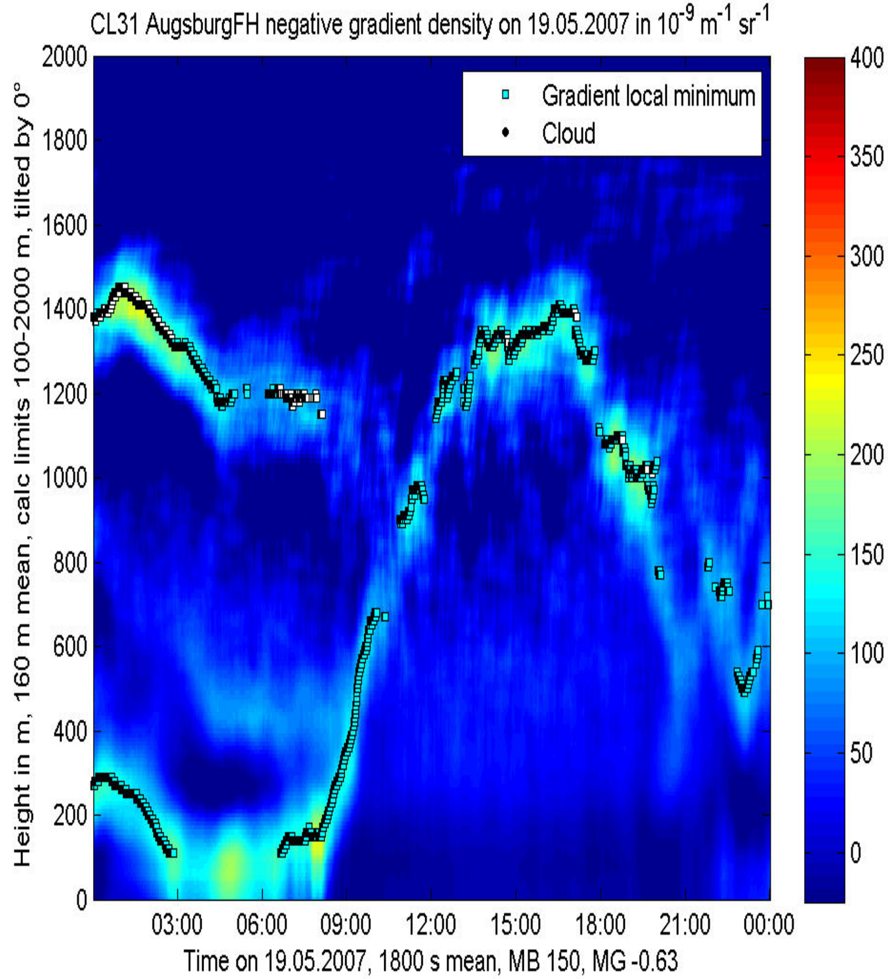

stefan.emeis@kit.edu Institute for Meteorology and Climate Research – Atmospheric Environmental Research

Algorithm to detect MLH from Ceilometer-Daten

criterion

minimal vertical gradient of backscatter intensity (the most negative gradient)

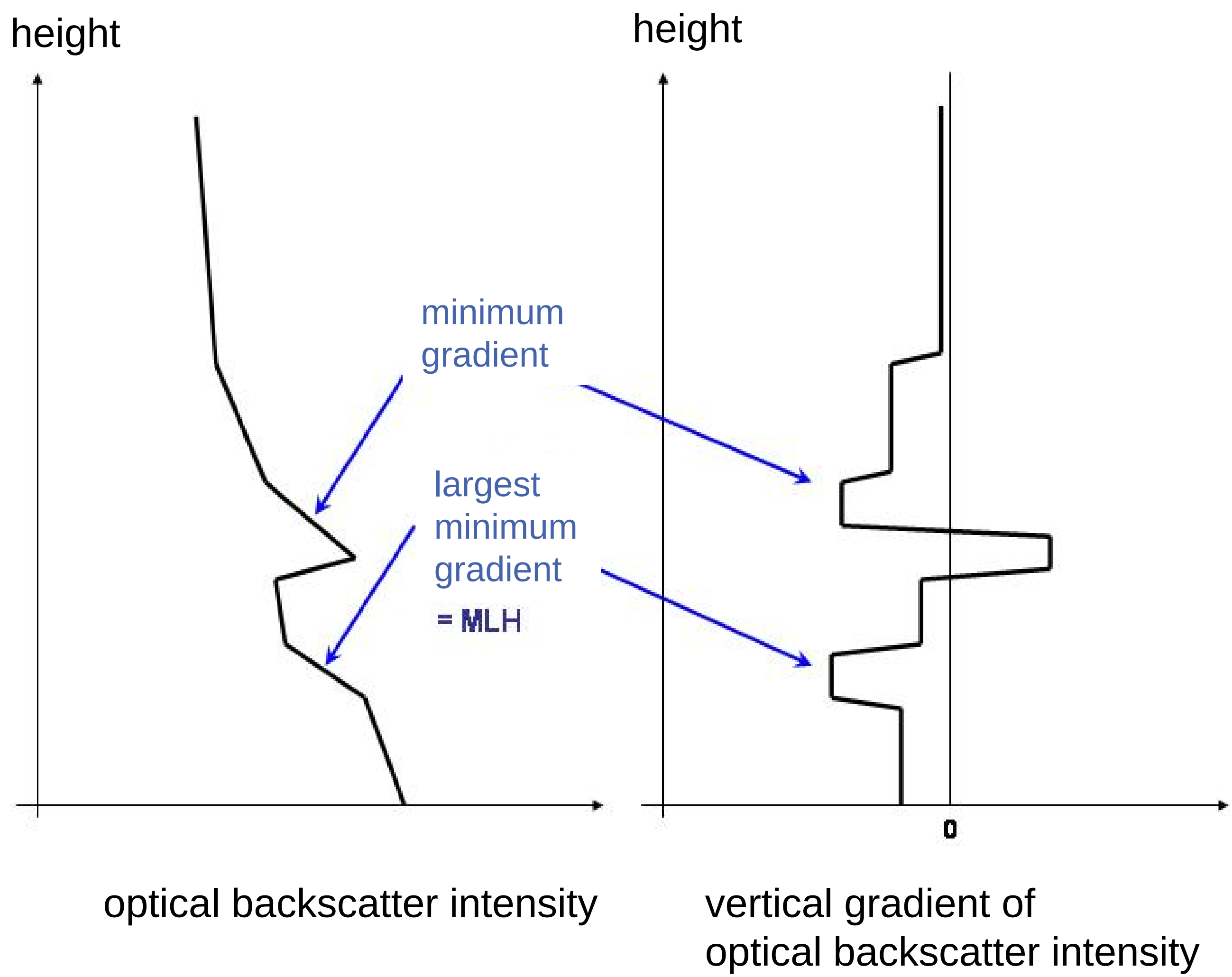

stefan.emeis@kit.edu Institute for Meteorology and Climate Research – Atmospheric Environmental Research

Different gradient methods (see Sicard et al. 2006, BLM 119, 135-157)

logarithmic gradient minimum

gradient minimum

inflection point method
(minimum of 2nd derivative)

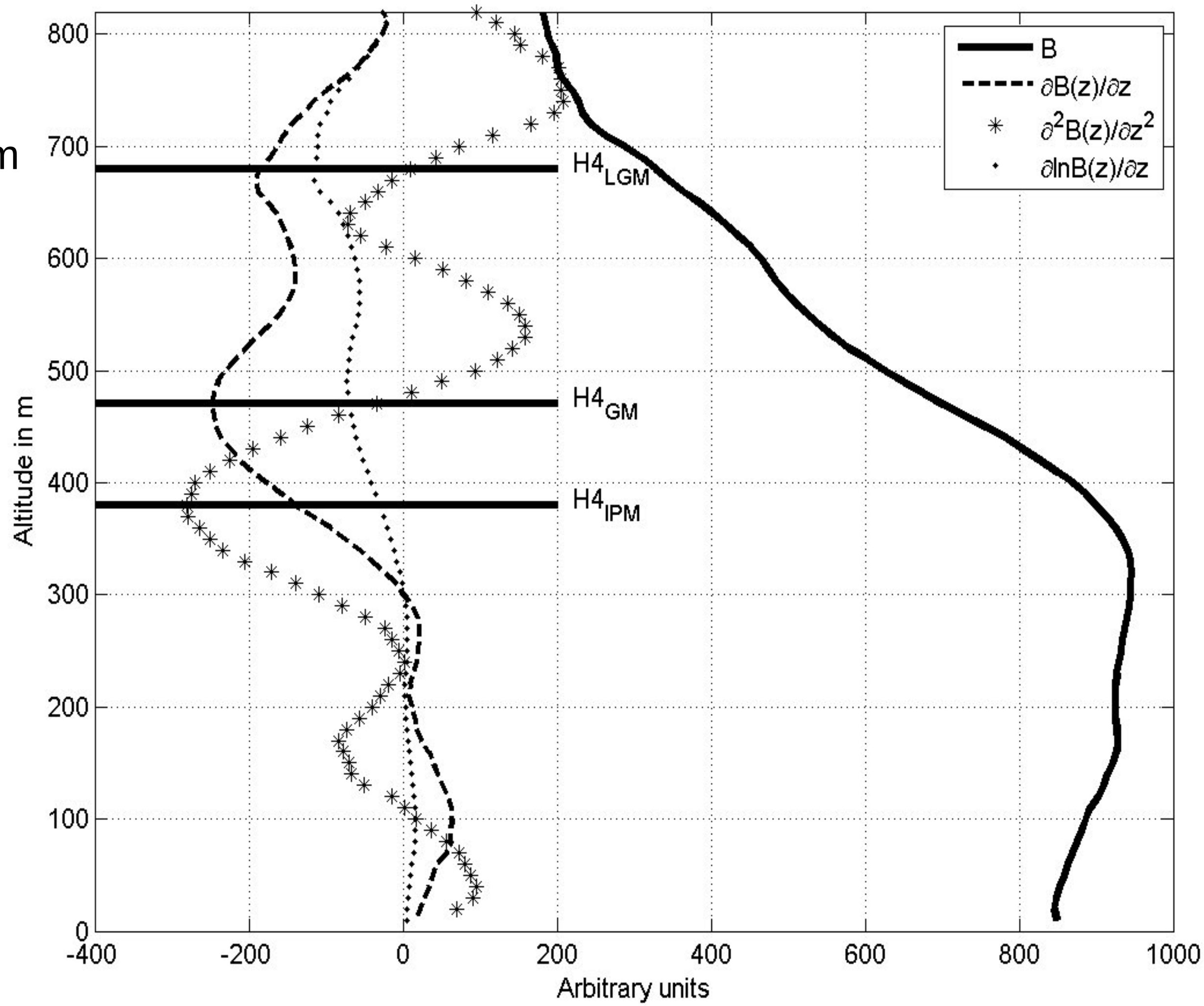

comparison of two different ceilometers

LD40

two optical axes

wave length: 855 nm

height resolution: 7.5 m

max. range: 13000 m

CL31

one optical axis

wave length: 905 nm

height resolution: 5 m

max. range: 7500 m

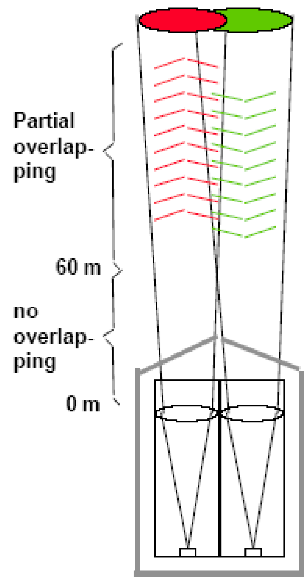

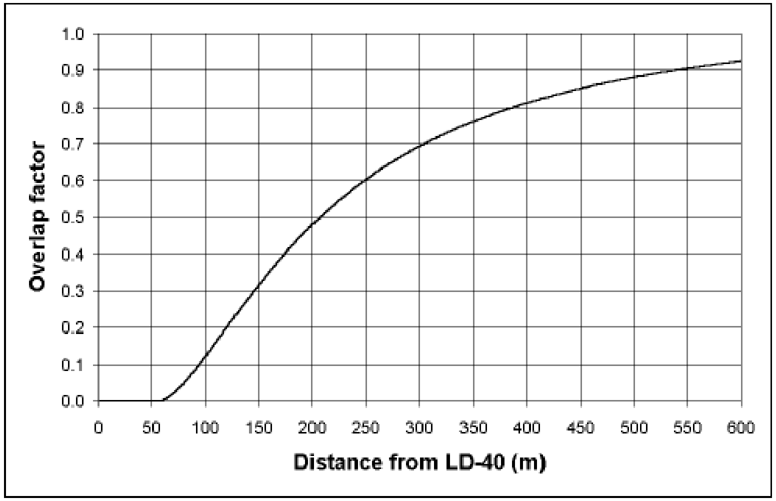

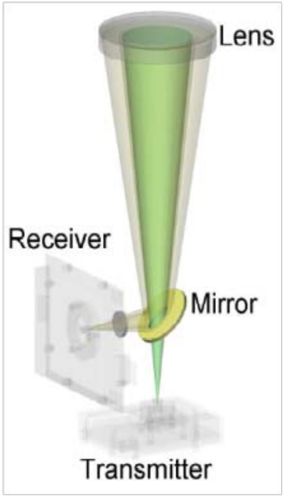

comparison of LD40 and CL31

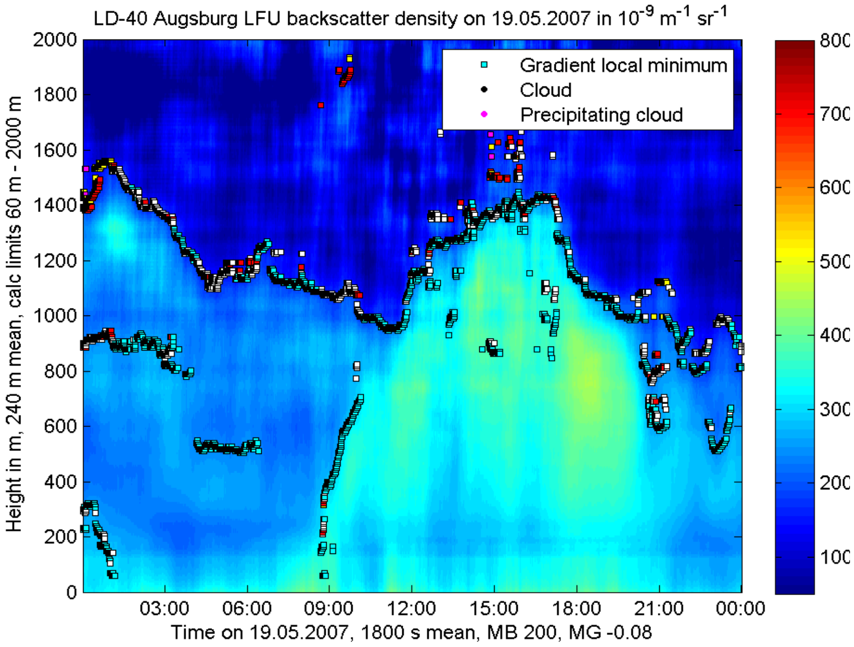

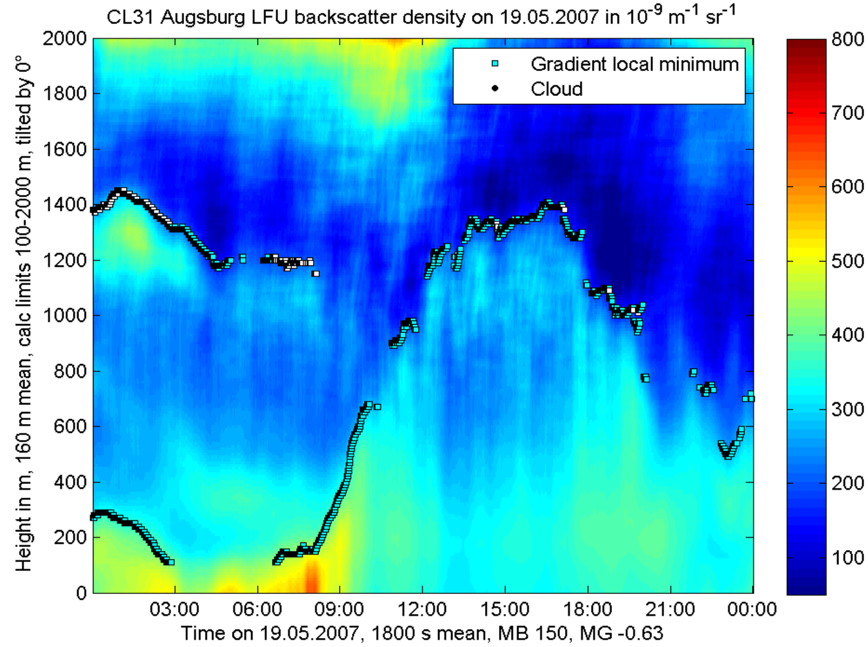

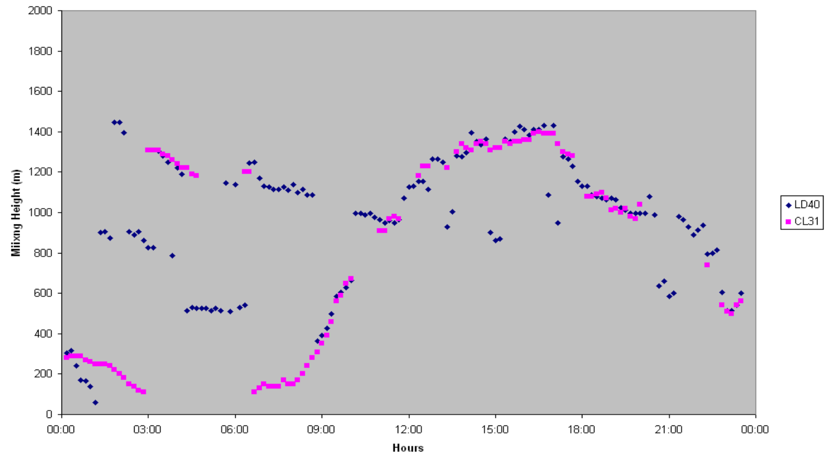

Eyjafjallajökull ash cloud over Southern Germany

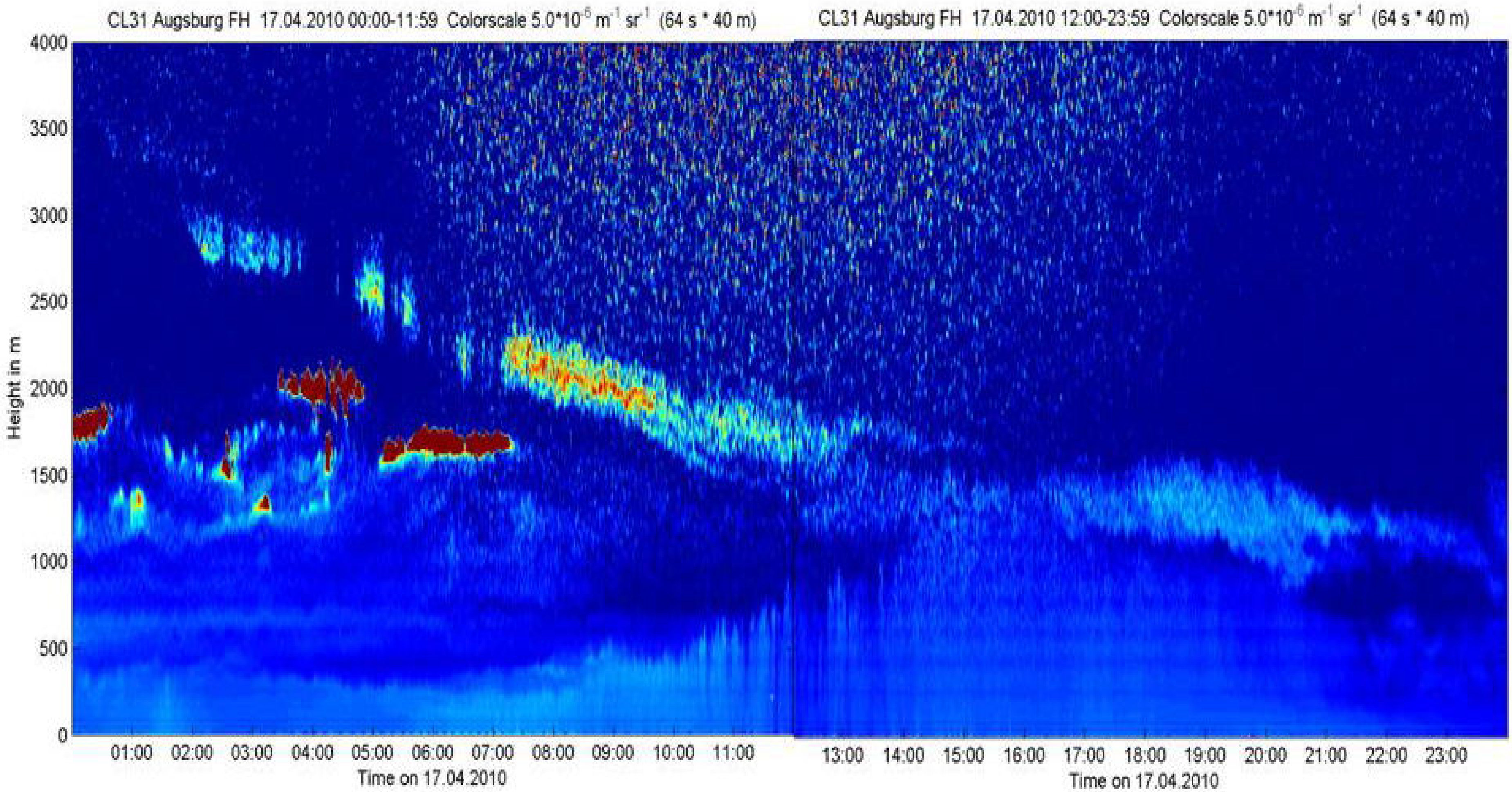

Doppler windlidar

wind, turbulence, aerosol detection, mixing-layer height

stefan.emeis@kit.edu Institute for Meteorology and Climate Research – Atmospheric Environmental Research

Doppler windlidar measuring principle

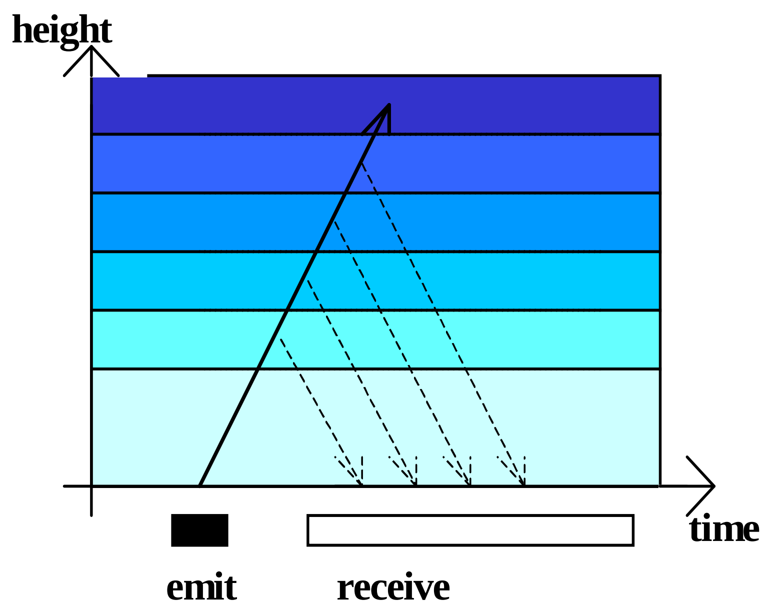

detection:

travel time of signal = height
backscatter intensity = particle size and number distribution
depolarisation = particle shape
Doppler-shift = wind speed in the line of sight

mobile Doppler windlidar from Halo Photonics

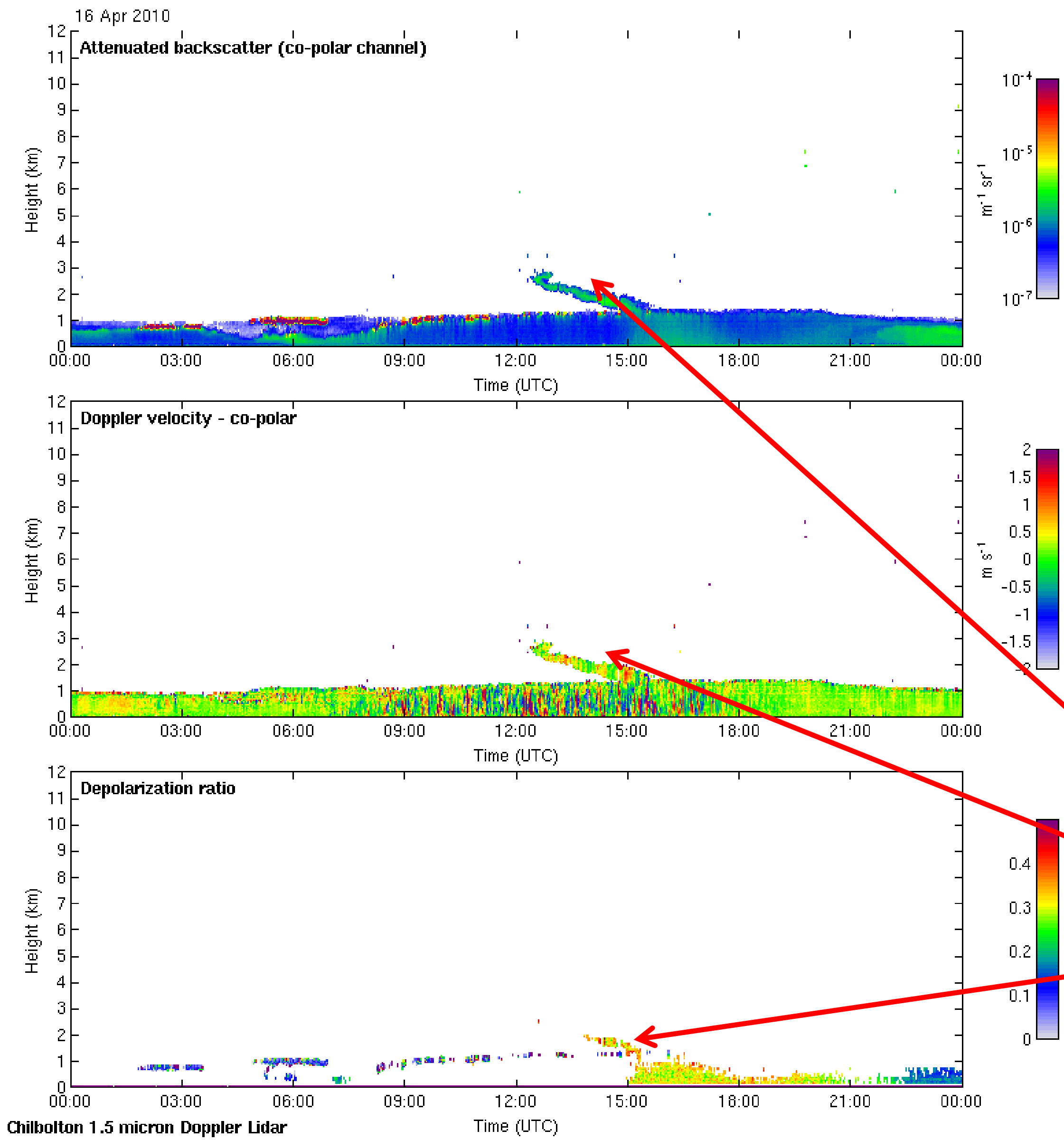

sample data from windlidar

April 16, 2010

by
Univ. of Reading

taken at

Chilbolton, UK

volcanic ash from Eyjafjallajokull

RASS

temperature, wind, turbulence, mixing-layer height

stefan.emeis@kit.edu Institute for Meteorology and Climate Research – Atmospheric Environmental Research

RASS (radio-acoustic remote sensing)

measures vertical temperature profiles

Bragg-RASS: windprofiler plus acoustic component

Doppler-RASS: SODAR plus electro-magnetic component

UHF RASS (boundary layer)

VHF RASS (troposphere)

stefan.emeis@kit.edu Institute for Meteorology and Climate Research – Atmospheric Environmental Research

RASS: frequencies

Bragg condition:
acoustic wavelength = ½ electro-magnetic wavelength

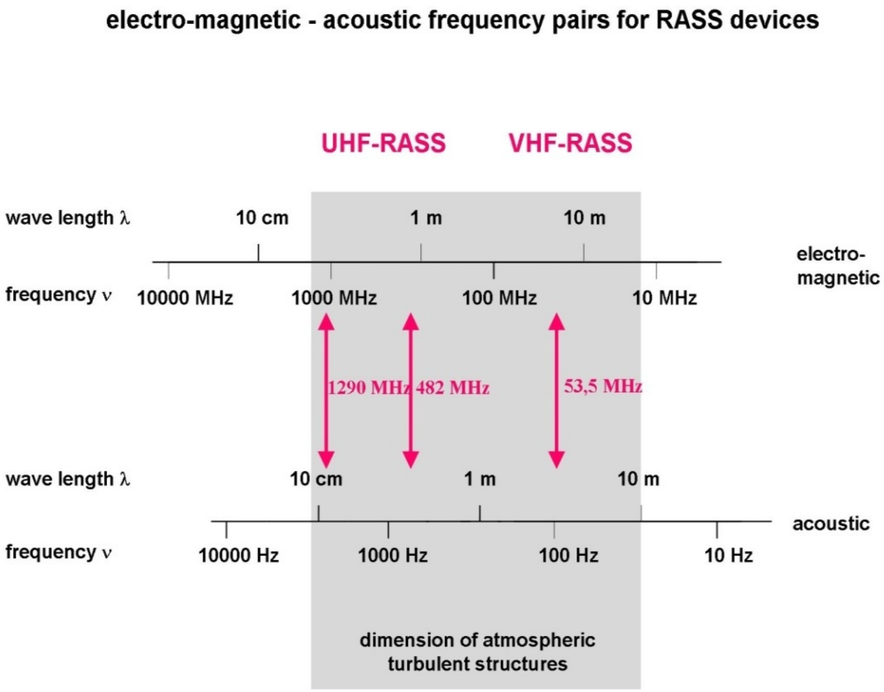

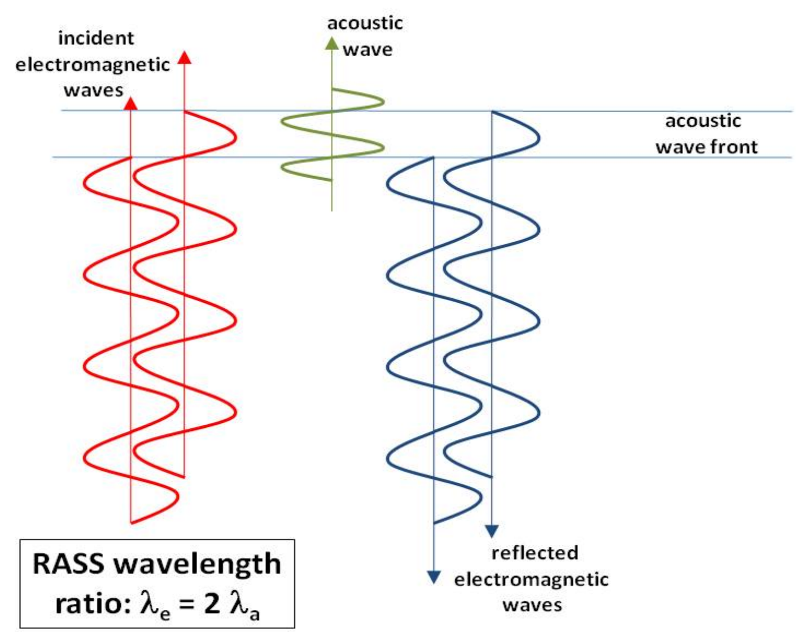

Emeis, S., 2010: Measurement Methods in Atmospheric Sciences - In situ and remote. Borntraeger, Stuttgart, 272 pp., 103 figs, 28 tables, ISBN 978-3-443-01066-9.

SODAR-RASS
(Doppler-RASS)

(METEK)

acoustic frequ.: 1500 – 2200 Hz
radio frequ.: 474 MHz
resolution: 20 m
lowest
range gate: ca. 40 m

vertical range: 540 m

Bragg-RASS

acoustic frequ.: about 3000 Hz
radio frequ.: 1290 MHz
resolution: 50 m
lowest
range gate: ca. 200 m

vertical range: 1000 m

example RASS data: summer day
potential temperature (left), horizontal wind (right)

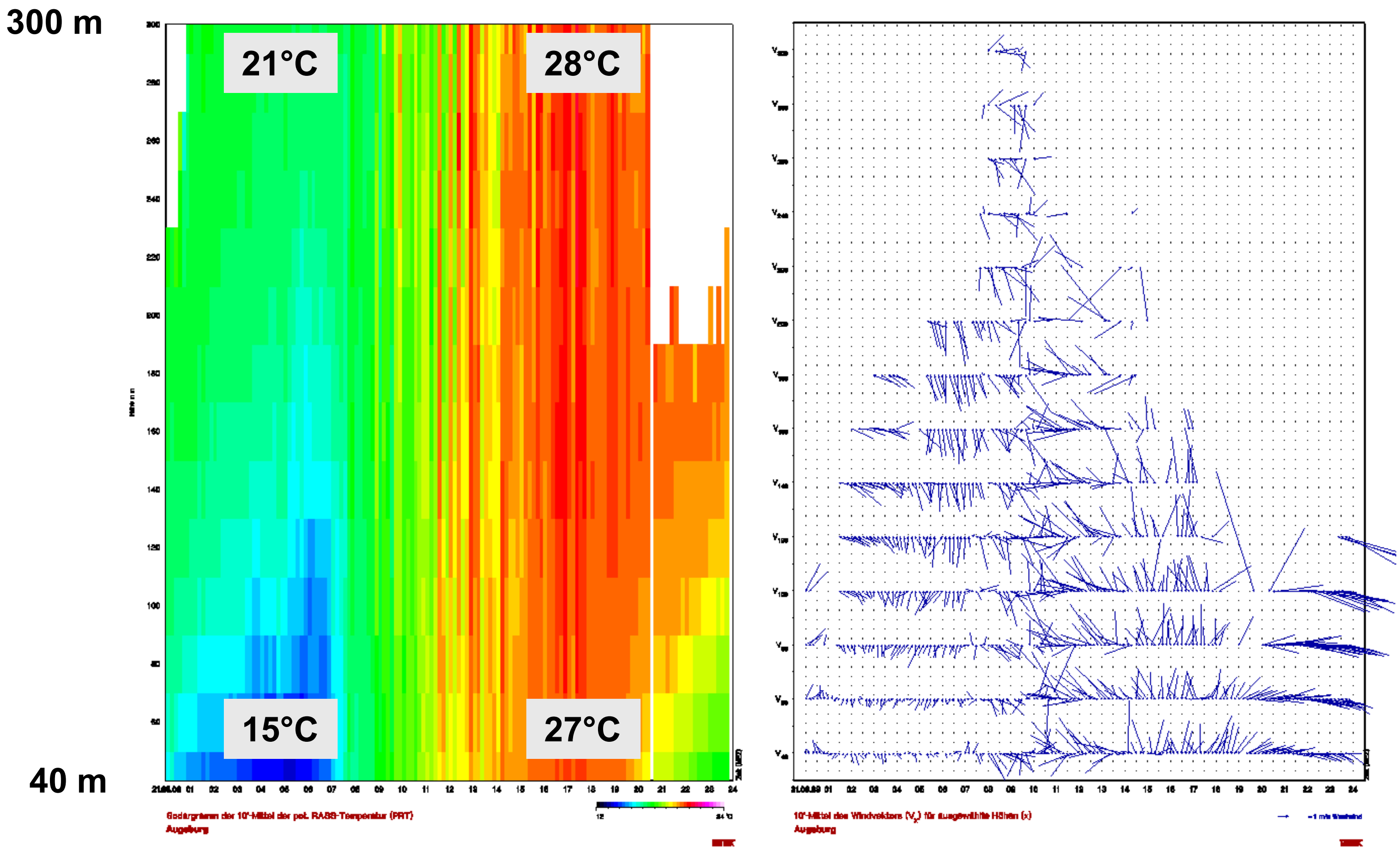

stefan.emeis@kit.edu Institute for Meteorology and Climate Research –
Atmospheric Environmental Research

example RASS data: winter day
potential temperature (left), horizontal wind (right)

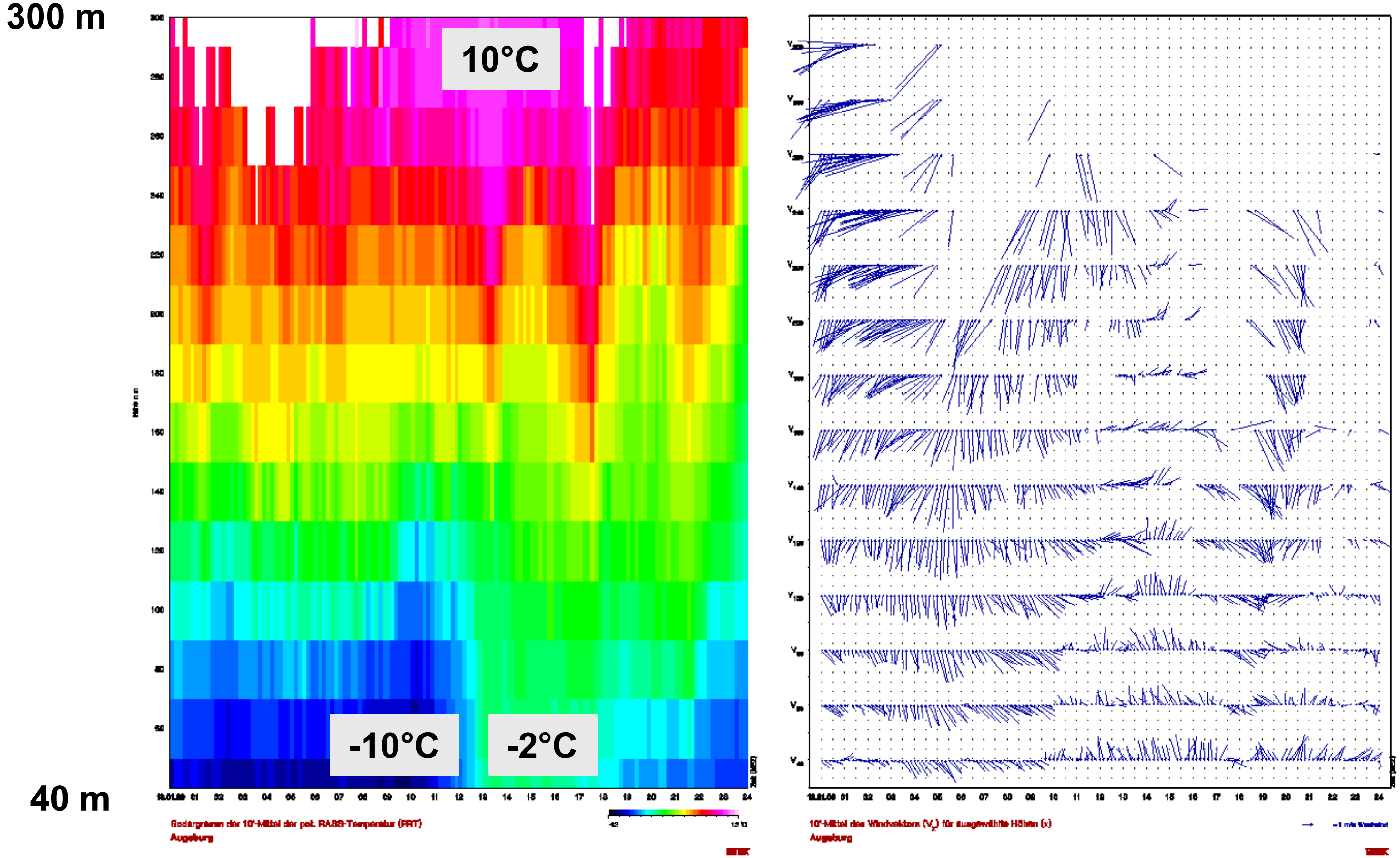

example RASS data: inversion
potential temperature (left), horizontal wind (right)

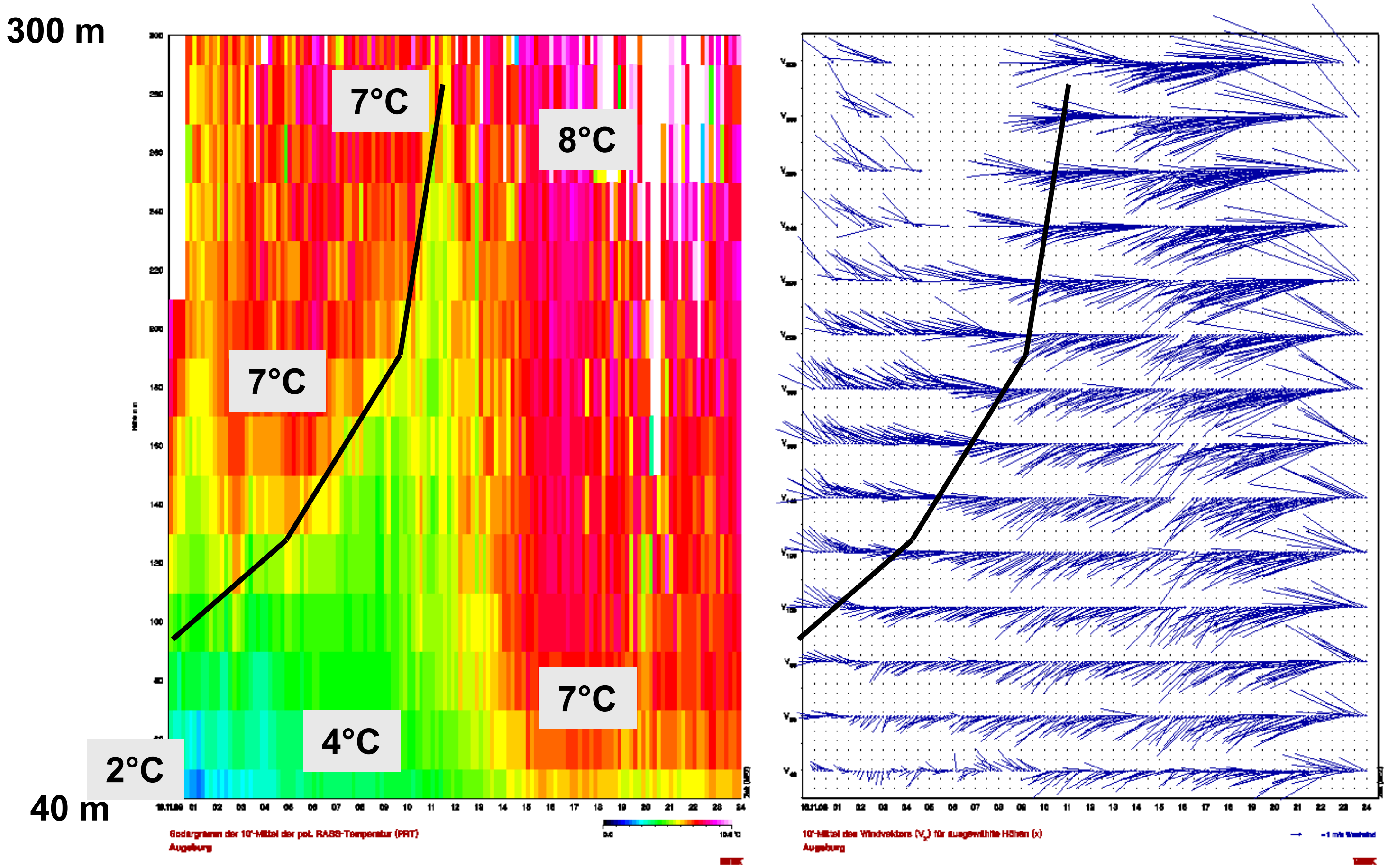

stefan.emeis@kit.edu Institute for Meteorology and Climate Research – Atmospheric Environmental Research

temperature profile and pollution

comparison of RASS data (potential temperature, right) with aerosol backscatter from a ceilometer (left)

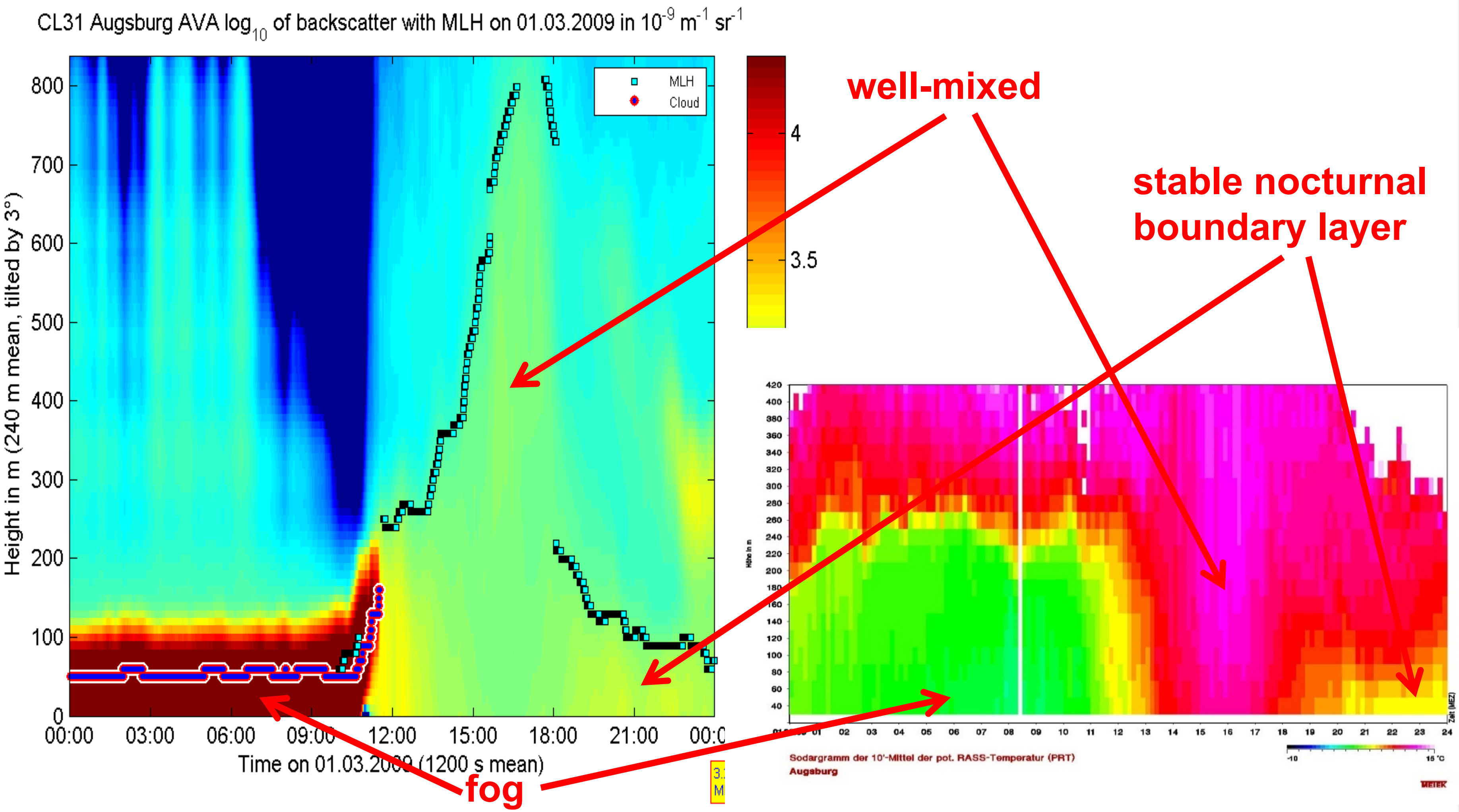

 stefan.emeis@kit.edu Institute for Meteorology and Climate Research – Atmospheric Environmental Research

RASS data Augsburg February 2009

potential temperature (top), backscatter SODAR (middle), Ceilometer (bottom)

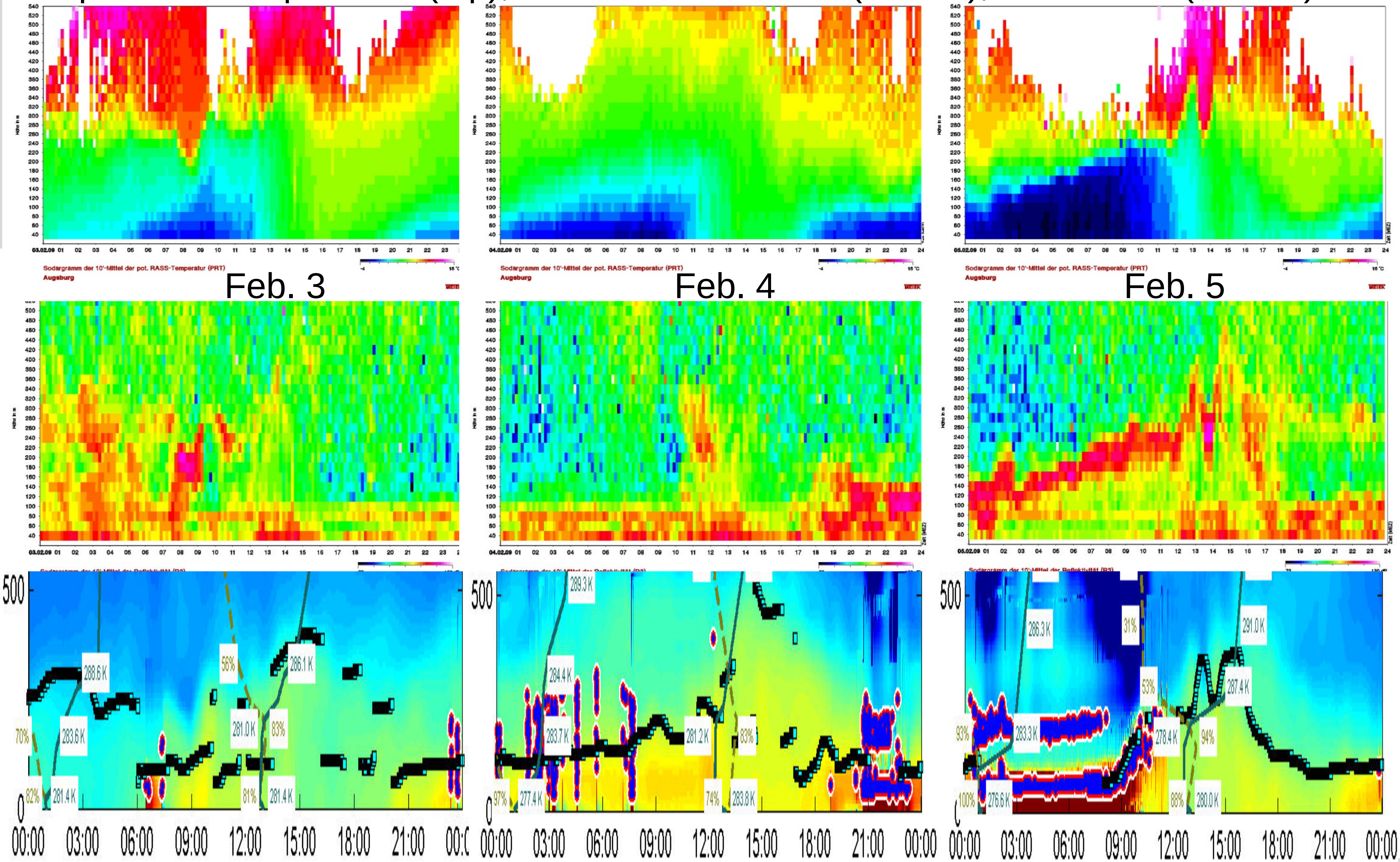

stefan.emeis@kit.edu Institute for Meteorology and Climate Research – Atmospheric Environmental Research

RASS data Augsburg February 2009

potential temperature (top), MLH RASS (middle), MHL SODAR/Ceilo (bottom)

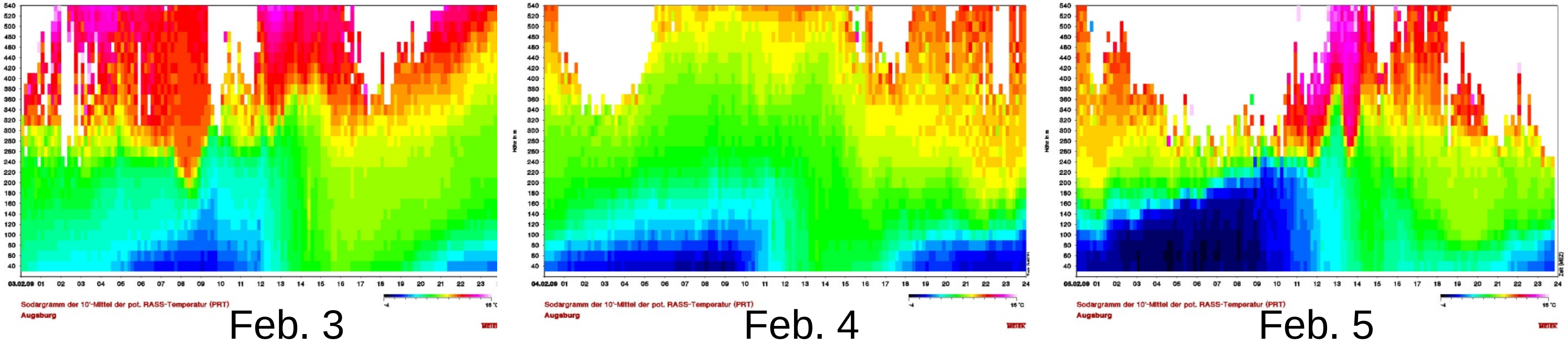

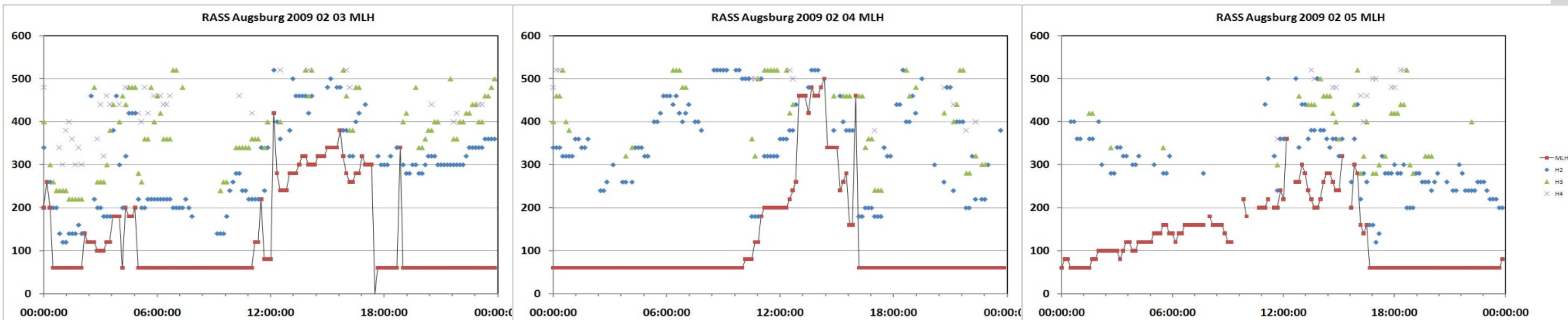

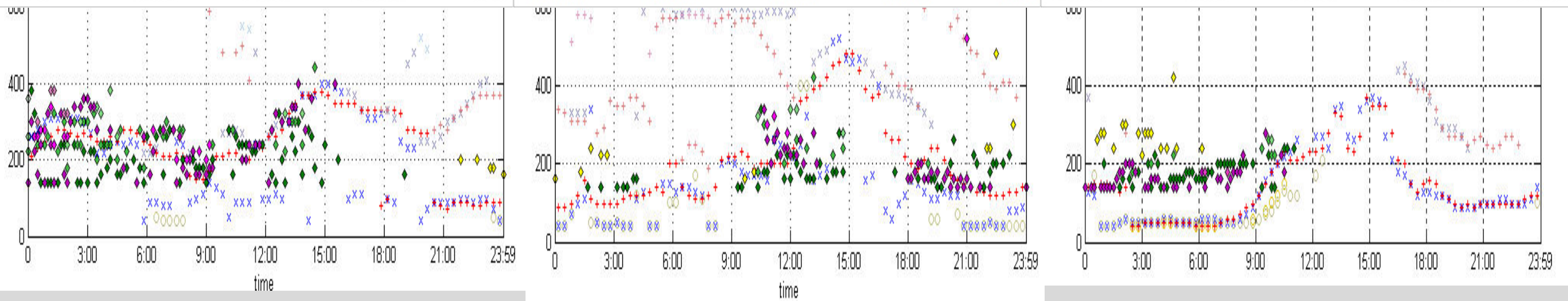

Summary

Conclusions:

☺ ☺ ☺ 💣 **RASS** **directly delivers temperature profiles, MLH, inversions, and stable layers can easily be detected, wind profiles are additionally available.**
Does not work properly **under high wind speeds. Restricted range.**

☺ ☺ 💣💣 **Ceilometer/windlidar** **detects aerosol distribution and water droplets. It has to be assumed that the aerosol follows the thermal structure of the atmosphere. Inversions and MLH can indirectly be inferred with a MLH algorithm. Wind from windlidar.**
Does not work properly **in extreme clear (aerosol-free) air and during precipitation events and fog.**

☺ 💣💣💣 **SODAR** **detects temperature fluctuations and gradients, but no absolute temperature. Inversions and stable layers can indirectly be inferred with a MLH algorithm. Wind and turbulence.**
Does not work properly **under perfectly neutral stratification, with very high wind speeds, and during stronger precipitation events. Restricted range.**

Literature

stefan.emeis@kit.edu Institute for Meteorology and Climate Research – Atmospheric Environmental Research

SODAR:

Asimakopoulos, D.N., C.G. Helmis, J. Michopoulos, 2004: Evaluation of SODAR methods for the determination of the atmospheric boundary layer mixing height. - Meteor. Atmos. Phys. 85, 85–92.

Beyrich, F., 1997: Mixing height estimation from sodar data – a critical discussion. - Atmos. Environ. 31, 3941–3953.

Ceilometer:

Schäfer, K., S.M. Emeis, A. Rauch, C. Münkel, S. Vogt, 2004: Determination of mixing-layer heights from ceilometer data. In: Remote Sensing of Clouds and the Atmosphere IX. Schäfer, K., A. Comeron, M. Carleer, R.H. Picard, N. Sifakis (Eds.), Proc. SPIE, Bellingham, WA, USA, Vol. 5571, 248–259.

Sicard, M., C. Pérez, F. Rocadenbosch, J.M. Baldasano, D. García-Vizcaino, 2006: Mixed-Layer Depth Determination in the Barcelona Coastal Area From Regular Lidar Measurements: Methods, Results and Limitations. - Bound.-Lay. Meteor. 119, 135–157.

RASS:

Engelbart, D.A.M., J. Bange, 2002: Determination of boundary-layer parameters using wind profiler/RASS and sodar/RASS in the frame of the LITFASS project. Theor. Appl. Climatol. 73, 53–65.

Emeis, S., K. Schäfer, C. Münkel, 2009: Observation of the structure of the urban boundary layer with different ceilometers and validation by RASS data. Meteorol. Z., 18, 149-154. (Open access, freely available from http://dx.doi.org/10.1127/0941-2948/2009/0365)

Reviews:

Emeis, S., K. Schäfer, C. Münkel, 2008: Surface-based remote sensing of the mixing-layer height – a review. - Meteorol. Z., 17, 621-630. (Open access, freely available from http://dx.doi.org/10.1127/0941-2948/2008/0312)

Emeis, S., M. Harris, R.M. Banta, 2007: Boundary-layer anemometry by optical remote sensing for wind energy applications. - Meteorol. Z., 16, 337-347.

Books:

Emeis, S, 2010: Measurement Methods in Atmospheric Sciences. In situ and remote. Series: Quantifying the Environment, Vol. 1. Borntraeger Stuttgart. XIV+257 pp., 103 Figs, 28 Tab. ISBN 978-3-443-01066-9.

Emeis, S, 2011: Surface-Based Remote Sensing of the Atmospheric Boundary Layer. Series: Atmospheric and Oceanographic Sciences Library, Vol. 40. 1st Edition., X+174 pp. 114 illus., 57 in color., H/C. ISBN: 978-90-481-9339-4, e-ISBN 978-90-481-9340-0, ISSN 1383-8601, DOI: 10.1007/978-90-481-9340-0

Thank you very much for your attention